A Hyperspectral Fluorescence Imaging System for Biological Applications

Guido Zavattini, *Member IEEE*, Stefania Vecchi, Richard M. Leahy, *Senior Member IEEE*, Desmond J. Smith, Simon R. Cherry, *Senior Member IEEE*

Abstract— **We are developing a hyperspectral imaging system aimed at imaging fluorescent molecules in two different contexts: *In vivo* 3-D molecular imaging of mice and multi-fluorophore imaging of 2-D tissue samples.**

The main concept is to add high resolution spectral information to the intensity data to improve imaging capabilities. The system is based on an imaging spectrograph, ImSpector, coupled to a CCD camera.

The system has been characterized and calibrated. Spectral imaging of tissue samples stained with fluorescent dyes has been performed to validate the principle and the 2-D imaging capabilities.

Near infrared 3-D in vivo fluorescence tomography is based on the intensity and spatial distribution of the fluorescent light reaching the surface of the animal as a function of the localized external excitation position. Based on the fact that the absorption coefficient of tissue is wavelength dependent, the measured spectrum of the fluorescent light will provide additional information, thus allowing an improvement of the 3-D reconstruction. By using solely spectral data we have demonstrated the capability of determining the 3-D position of a localized source within a red meat phantom.

I. Introduction

The aim of the system we are developing is to address two important challenges in biomedical imaging: 3-D *in vivo* near infrared fluorescence imaging of mice; 2-D multi-fluorophore imaging of thin tissue sections.

A. 3-D in vivo fluorescence imaging of mice

3-D fluorescence imaging of mice is an emerging imaging technique. The concept is that near infrared light is highly diffused and only slightly absorbed by tissue, allowing a measurable amount of light, emitted by fluorescent molecules marking a biological agent in a mouse, to be detected on its surface. Recent work has shown that with appropriate external illumination, 3-D reconstruction of localized fluorescence is possible [1]. The technique is based on measuring the light spot reaching the surface of the mouse as a function of an external localized illumination typically performed with a laser.

In this work we propose to introduce spectral information in the detected light so as to add an independent data set hence improving the 3-D reconstruction.

The idea is based on the fact that the absorption coefficient of tissue is wavelength dependent and the measurement of the wavelength spectrum allows the determination of the depth of a localized fluorescent object.

A spectral imaging apparatus has been assembled and some test measurements on red meat phantoms have been performed demonstrating the depth dependence of the detected wavelength spectrum.

B. 2-D multi-fluorophore imaging of tissue samples

Multiplexed fluorescent imaging of 2-D tissue slices is limited to a maximum of about 3 different fluorophores using traditional techniques based on excitation/emission filters. The difficulty in this case is that the emission filters and excitation filters for the different fluorescent molecules must be mutually exclusive.

With a hyperspectral imaging device it is possible to acquire highly overlapping spectra and to unmix the different components, thus allowing a greater number of different dyes to be imaged. Furthermore the advent of quantum dots, with narrower emission spectra, a wide range of emission wavelengths, all excitable with a single blue wavelength opens up the possibility of much higher degrees of multiplexing than was previously possible.

II. Apparatus

The system is based on an imaging spectrograph, ImSpector, (Model V10E, Specim, Oulu, Finland; www.specim.fi) which can image a line in the object space into a 2-D spatial and wavelength image. This image is then acquired with a CCD camera. By scanning the spectrograph across the object one can therefore acquire a 3-D volume with two of the dimensions being the spatial coordinates and the third being the wavelength. ImSpector has a wavelength band of 400-1000 nm, a slit length of 14.3 mm and a numerical aperture of f/2.4. The spatial resolution is 9 microns on the CCD image plane along the spatial direction whereas the wavelength resolution, determined by the slit width (25

G. Zavattini, S Vecchi, S. R. Cherry, Dept. of Biomedical Engineering, University of California-Davis, Davis, CA, USA; R.M. Leahy, Signal and Image Processing Institute, University of Southern California, Los Angeles, CA, USA; D. J. Smith, Department of Molecular and Medical Pharmacology, UCLA School of Medicine, Los Angeles, CA, USA.

0-7803-8257-9/04/$20.00 © 2004 IEEE.

microns), is 2 nm. The CCD camera is a front illuminated 512x512 chip (Roper Scientific, Trenton, NJ), with 24 micron pixels, thermoelectrically cooled to –40˚C to reduce dark current noise. A front illuminated version was chosen to avoid etaloning effects present for wavelengths above 750 nm in back-thinned CCD chips. Three light sources have been implemented: 473 nm, frequency doubled Nd:YAG (doubling of the 946 nm line) 10 mW laser; a 532 nm frequency doubled Nd:YAG (doubling of the 1064 nm line) 7 mW laser; and a 640 nm, 5 mW laser diode with a 636.2 nm, 10 nm interferometric narrow band filter to eliminate the spectral tails in the spectrum. The imaging system and light sources are mounted on translation stages with a 1 mm/rev. screw and are controlled by 400 steps/rev stepper motors.

According to the laser used, two interferometric filters can be placed in front of the imaging device to eliminate the excitation line: a 500 nm long pass filter (Chroma Technology Corp., Rockingham, VT, USA) and a 2-line (532 nm and 640 nm) rugate notch filter (Barr Associates, Westford MA, USA). A figure of the optical density of the two filters is shown in Figure 1.

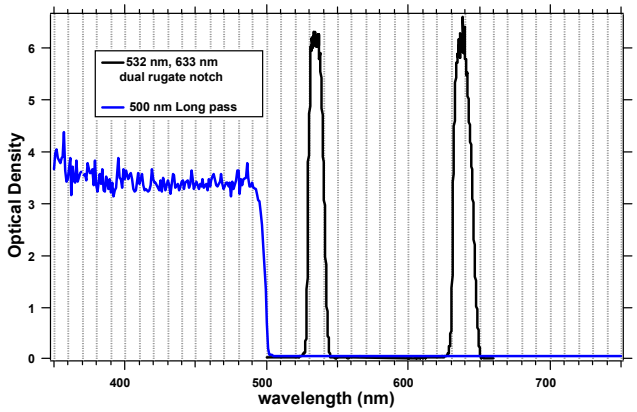

Figure 1: Optical density of the 500 nm long pass filter and the 2-line rugate notch filter.

Depending on the imaging task, the geometry of the illumination can be changed from a line, for tissue samples, to a matrix of points on the object for the 3-D imaging. In this second configuration the laser is placed on an X-Y translation system with analogous characteristics as for the imaging system. In 3-D imaging the illumination of the mouse is performed from underneath and the imaging from above.

Given the object size, the objective chosen was a 17 mm focal length, f/1.4, corrected from 400 – 1000 nm (Schneider Optics, Hauppauge, NY). The system is mounted in a light-tight black box. A photograph of the system is shown in Figure 3.

III. Methods

The imaging capabilities, wavelength calibration and efficiency of the system were first investigated. Two different series of measurements were performed to understand the capabilities for the proposed applications.

A. Spectral dependence on tissue depth.

A first set of measurements was made to understand and assess the spectral variations of the detected fluorescent light as a function of thickness of traversed tissue. Four slices of red meat were used, each about 5 mm thick, and small fluorescent phantoms, with Vybrant DiD dye (Molecular Probes, Eugene, OR, USA, peak excitation = 640 nm, peak emission = 675 nm), were placed between the slices at different depths. Two sets of measurements were taken: One with the Vybrant DiD fluorescence samples in place, and one without. This second measurement was taken to evaluate the auto fluorescence of the meat sample. The position of the 5 fluorescent samples is shown in Figure 2.

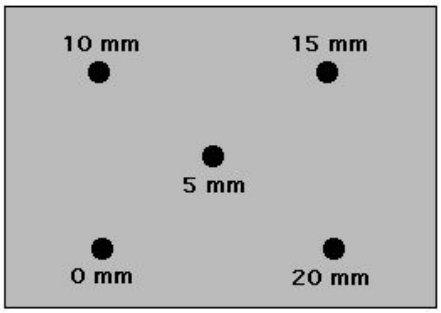

Figure 2: Schematic diagram showing the position of the 5 fluorescent samples placed at different depths within the red meat phantom.

The slices were placed flat down, illuminated from underneath and imaged from above. The illumination was performed on a 9 by 5 grid of points, each 1 cm apart. For each illumination point, the spectrograph was scanned across the meat phantom in 1 mm steps for a total of 4 cm. For each position a 512 spatial bins x 120 spectral bins image was acquired. The spectral bins corresponded to a band from 621.3 nm to 898.4 nm. In this way a data set of 9x5 hyperspectral images each consisting of 512x40 spatial bins times 120 spectral bins was acquired. The setup in this configuration is shown in Figure 3.

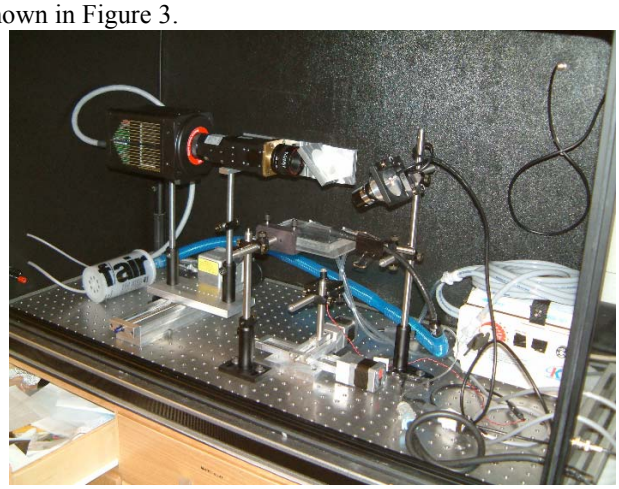

Figure 3: Photograph of the hyperspectral imaging system being developed at UC Davis.

Our principle interest was to study the spectral dependence of the fluorescence signal as a function of tissue depth.

Therefore the spectra were extracted for each of the 512x40 image pixels and the ratio, *R,* of two wavelength bands (denoted as 'Low' and 'High' in Figure 8) were taken generating 9x5 images of *R*. The higher wavelength band was used for normalization, as its shape did not vary appreciably as a function of source depth.

From 5 of the 45 images, corresponding to the 5 laser positions nearest to the 5 fluorescent sources, a calibration of *R* versus source depth was extracted. This calibration was then used in all the images to determine the 3-D spatial coordinates of the 5 fluorescent samples.

B. 2-D multi-fluorophore imaging.

The possibility of unmixing highly overlapping spectra was first studied by printing a phantom on a transparency with an inkjet printer. Two of the colors in the cartridge were substituted with Vybrant DiD and Vybrant DiR dyes. In addition to the dyes, both the transparency and the black ink had a fluorescence emission. The printed pattern and the spectra of the 4 components are shown in Figure 4. The printed area is 2.5 mm wide and 9 mm high. In this study the excitation was done with the 640 nm laser and with the dual rugate notch filter in place and the spectrograph was scanned across the phantom in 100 μm steps.

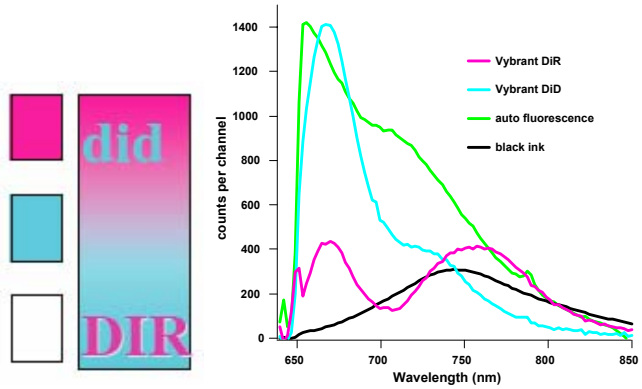

Figure 4: Pattern printed with an inkjet printer where the magenta color (dark grey) was substituted with Vybrant DiR dye and the cyan color (light grey) was substituted with Vybrant DiD dye. On the right are the spectra of the 4 different components: Vybrant DiD, Vybrant DiR, black ink, and the auto fluorescence of the transparency.

Given a hyperspectral image, $\mathbf{S}_{\lambda}^{x,y}$, with x and y denoting the spatial coordinates and λ the wavelength, and a set η of reference spectra, $\mathbf{M}_{\lambda,\eta}$, the image, $\mathbf{W}_{\eta}^{x,y}$, of each spectral component can be obtained by inverting the expression

$$S_{\lambda}^{x,y} = M_{\lambda,\eta} W_{\eta}^{x,y}$$

In this work the inversion was performed by fitting the measured spectrum for each x,y coordinate of the hyperspectral data with the four spectral components.

The same technique was applied on a 40 μm thick slice of a transgenic mouse expressing green fluorescent protein (GFP) to evaluate the technique. Two small samples of quantum dots were superimposed on the mouse slice. The quantum dots used in this example emitted at 655 nm and 525 nm. The excitation in this case was obtained with the 473 nm blue laser and with the 500 nm long pass filter in place.

IV. RESULTS

A. Calibration and characterization

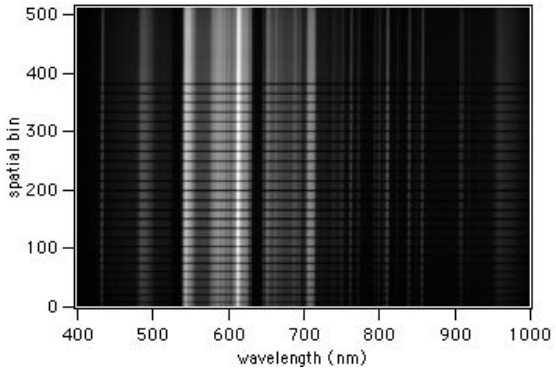

Figure 5: Image obtained with ImSpector of a white piece of paper with black lines and illuminated with a fluorescent lamp.

Figure 5 shows a typical image obtained using ImSpector when imaging a piece of white paper with black lines across it. On the x-axis is the wavelength and on the y-axis the spatial coordinate. The vertical lines are due to the spectrum of the ambient light (fluorescent lamps). Figure 6, left, shows a horizontal profile at spatial bin 400 of Figure 5 showing the wavelength spectrum. Figure 6, right, shows a measurement of the relative efficiency of the system (lens, ImSpector, notch filter, CCD).

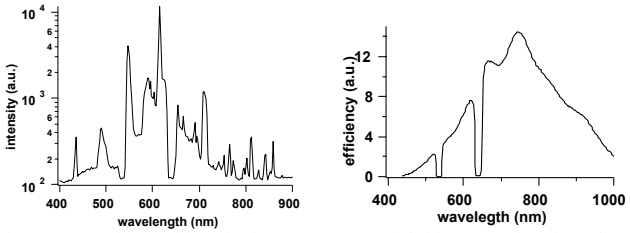

Figure 6: Left, profile of Figure 5 at spatial bin 400 showing the line structures. Right, measured relative efficiency of the system showing the two rejection bands of the notch filters at 532 nm and 640 nm.

B. Spectral dependence on tissue depth.

As an example the fluorescence image of the 15 mm deep source is shown in Figure 7

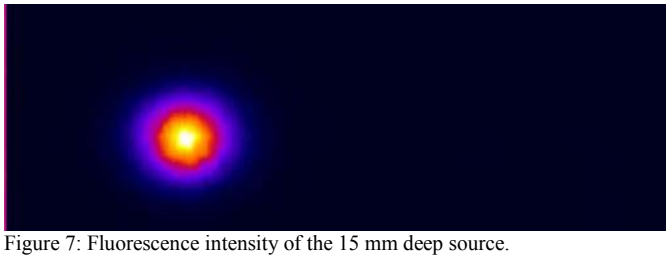

Figure 7: Fluorescence intensity of the 15 mm deep source.

The normalized spectra of the five sources taken at their most intense image pixel are shown in Figure 8, top, and the

calibration of *R* as a function of depth is given in Figure 8, bottom, superimposed with an exponential fit.

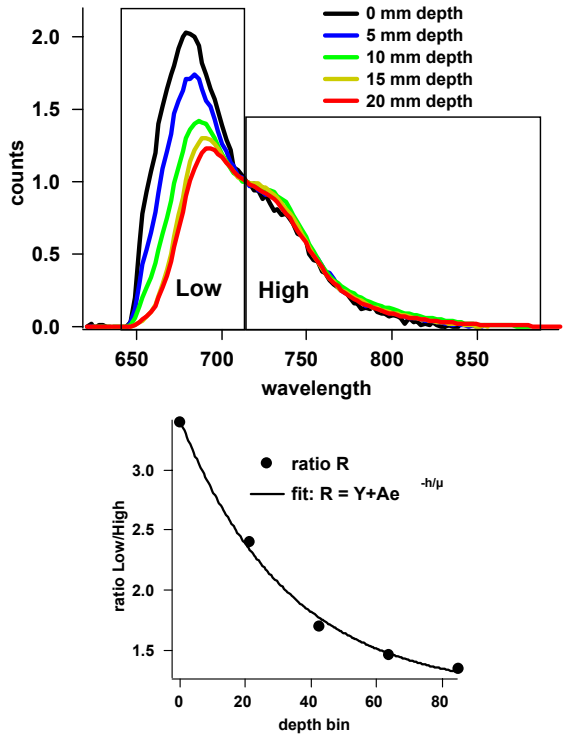

Figure 8: Top: Wavelength spectra for fluorescence light reaching the tissue surface from different depths. Bottom: Ratio *R* plotted as a function of depth.

In Figure 9 is the pseudoimage of the ratio *R* for the same source. The lower is the value of *R*, the more has the 'Low' component of the spectrum been absorbed relative to the 'High' component and therefore the farther has the light traveled within the tissue. Indeed the maximum value of *R* is at the center of the spot where the source is nearest to the surface of the phantom. As one can see in Figure 9, by moving away from the center of the spot the value of *R* decreases because the source-surface distance increases.

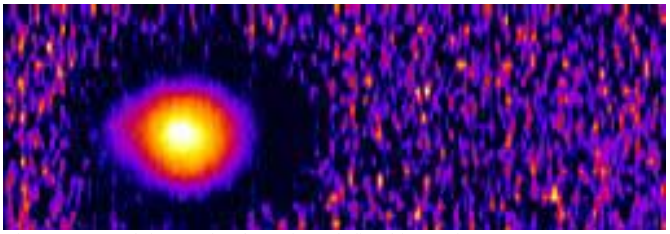

Figure 9: Pseudoimage for the ratio *R* defined in section IIIA.

Given the simple slab geometry of the phantom, the 2-D spot profiles were fit with a function of the form

$$R = Y + Ae^{-\sqrt{(x-x_0)^2+(y-y_0)^2+z_0^2}/\mu}$$

where the term $\sqrt{(x-x_0)^2+(y-y_0)^2+z_0^2}$ represents the distance from the source at position (x_0, y_0, z_0) to the surface of the phantom at (x, y, 0). The value of μ was taken from the calibration whereas Y, A and (x_0, y_0, z_0) were left as parameters.

In Figure 10 one can see the 3-D reconstruction of the 5 sources solely from the spectral information.

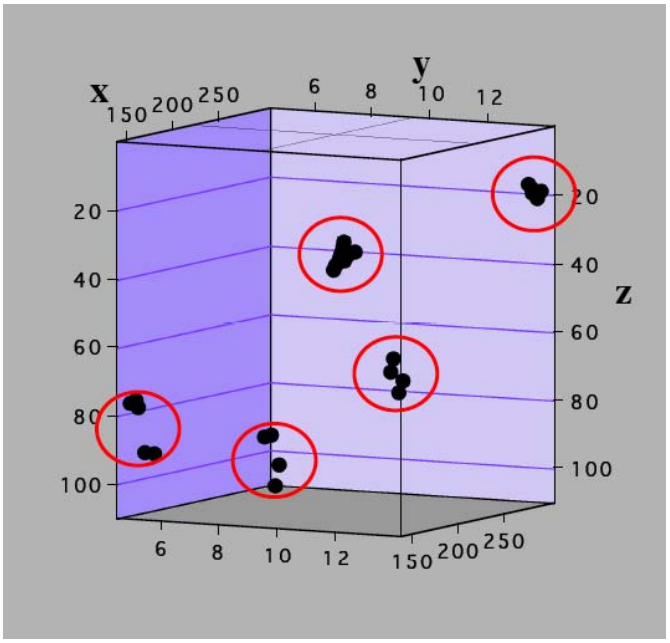

Figure 10: Reconstructed positions of the 5 fluorescent sources obtained solely from the spectral information.

C. Multiple fluorophore 2-D imaging

The result from imaging the printed phantom is shown in Figure 11. Each figure represents one of the four spectral components unmixed as described above.

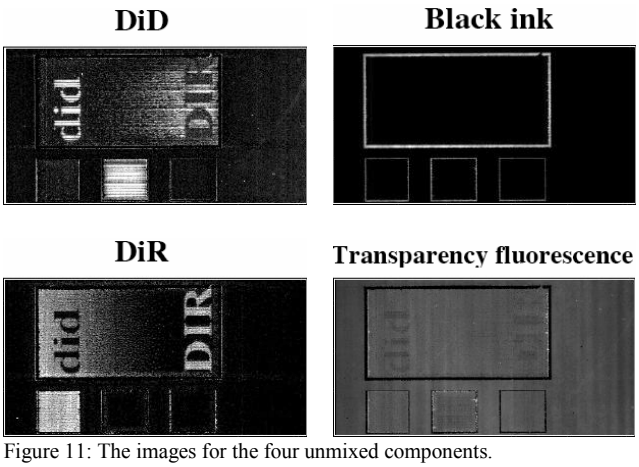

Figure 11: The images for the four unmixed components.

The images show that the technique works well. The black line in the image of the auto fluorescence is due to the absorption of the emitted light by the overlapping and opaque black ink.

The results from imaging the mouse slice are shown in Figure 12. Again 4 components were unmixed: GFP, auto fluorescence from the tissue, quantum dot 655 and quantum dot 525. The measured spectrum, shown with grey markers, is superimposed with the global fit. The graphs also show in blue the GFP component, in red the quantum dot 655 nm component and in green the quantum dot 525 nm component.

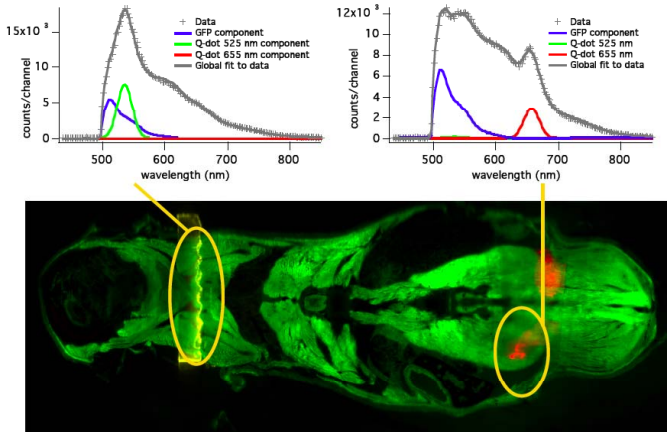

Figure 12: Image of a mouse slice superimposed with quantum dots emitting at 655 nm and 525 nm. Top: Spectrum of two different regions where the different emissions are simultaneously present. In grey are the data points superimposed with the global fit whereas in the different colors are the GFP, qdot655 and qdot525 components.

V. CONCLUSIONS

A hyperspectral imaging system has been assembled and first images have been acquired. These first measurements demonstrate the validity of using hyperspectral data for providing information on source depth in 3-D imaging, and for separating multiple fluorophores in 2-D tissue sample imaging.

[1] **Ntziachristos** V, Weissleder R. "Charge-coupled-device based scanner for tomography of fluorescent near-infrared probes in turbid media." *Medical Physics,* vol.29, no.5, May 2002, pp.803-9.